Nonuniversal conductivity exponents in continuum percolating Gaussian fractures

F. Flukiger, F. Plouraboué, and M. Prat

Institut de Mécanique des Fluides de Toulouse, U.M.R. C.N.R.S. - INP/UPS, N5502 Avenue du Professeur Camille Soula 31400 Toulouse, France

(Received 12 December 2007; revised manuscript received 7 February 2008; published 30 April 2008)

We study the electrical and hydraulic conductivity percolation exponents in a Gaussian fracture using the method proposed in Plouraboué *et al.* [Phys. Rev. E **73**, 036305 (2006)]. Nonuniversal conductivity percolation exponents are found: they differ from the theoretical predictions for infinite system size for frozen power-law distributions of local conductivities, as with their finite size corrections. In the hydraulic case, we also find that the probability density function of the conductivity follows a power-law distribution near the percolation threshold.

DOI: 10.1103/PhysRevE.77.047101 PACS number(s): 46.50.+a, 47.60.−i

I. INTRODUCTION

In this paper we study the electrical and hydraulic transport properties of a Gaussian fracture near the percolation threshold since this question has not been previously investigated for this particular continuum percolation system [2]. When the two rough surfaces forming the fracture are pressed together under the effect of an applied load, local gaps remain in between them due to imperfect matching. These local gaps form the so-called aperture field, which represents a continuous two-dimensional (2D) scalar description of the empty space left for a fluid to flow between the two solid surfaces. As illustrated in Fig. 1 for a smooth surface pressed onto a rough one, the local value of the aperture field is zero when two solid surfaces are in contact. As previously explained in [1] and illustrated in Fig. 1(b), this continuum problem can be mapped onto a discrete network of links. As a result, two intensive parameters can be used to describe the evolution of such systems: the normalized surface area, A, or the link fraction, p, which are normalized so that $0 \leq A \leq 1$ and $0 \leq p \leq 1$. The normalized surface area A is the ratio of the contact surface area to the total surface area, i.e., the relative surface contribution of closed regions of the aperture field [white regions in Fig. 1(b)]. Within the limit of pure plastic deformation of asperities, there is a simple relationship between the normal applied load W, and the contact area: $W=\Phi A$, where Φ is the Brinell hardness. At the percolation threshold, A reaches a critical value A_c and the mechanical hardness reaches a limit value when the leakage drops to zero according to a power law of the controlling parameter A_c-A. In previous studies on fractures [2], the open fractional area, i.e., $A_o=1-A$, is used to characterize the occupation probability of the system (A_o can be regarded as a site occupation probability).

The second parameter that is used is the network link fraction, p, which is the number of links in the discrete network divided by the total number of links when there is no contact between the two surfaces. The relationship between the link fraction and the surface geometry is more difficult to grasp. One has to realize that the major resistance to fluid flow is localized in constrictions associated with the aperture field saddle points. The resistance network is a random discrete bond network for which the distance to the percolation threshold p_c is evaluated through the traditional controlled parameter $\epsilon=p-p_c$. For the sake of completeness, we shall present the results using both ϵ and A_c-A.

II. RESULTS

A. Local conductance distribution near percolation threshold

We have previously shown, in Eq. (10) of [1], that the local conductances of the links are power-law distributed for small conductance values so that their probability density functions (PDF) fulfill $p(g_n) \sim g_n^{-(n-1)/n}$. In the case $n=1$ there is no singular behavior of the PDF. On the other hand, when

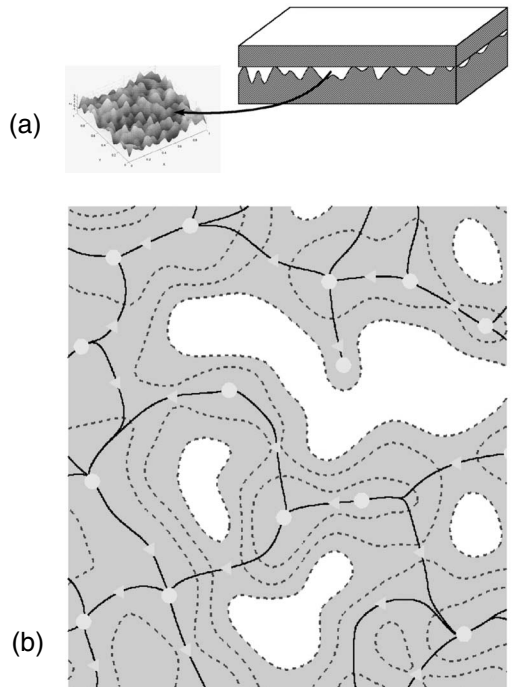

FIG. 1. (a) A 3D rough surface pressed onto a solid plane leaves empty spaces which form a 2D aperture field. (b) From this aperture field, it is possible to generate a discrete network of geodesics connecting the aperture maxima [1]. White regions are associated with regions of contact between the two surfaces where the local aperture is zero, while gray regions are those associated with nonzero aperture regions. Some level sets of the aperture map are represented with dotted curves in these gray regions. The geodesic network linking *maxima* is represented with continuous black lines, where the *maxima* are represented by gray filled circles. The saddle-point position along these geodesic networks are represented by triangles.

TABLE I. Coefficients of Eq. (1).

	(a)	
N	$a_\epsilon(N)$	$b_\epsilon(N)$
128	0.53	−0.86
256	0.60	−0.92
512	0.66	−1.04
1024	0.71	−1.10
2048	0.74	−1.11
	(b)	
N	$a_A(N)$	$b_A(N)$
128	0.111	8.8×10^{-3}
256	0.173	9.1×10^{-3}
512	0.214	9.3×10^{-3}

$n=3$, $p(g_3)\sim g_3^{-2/3}$ diverges algebraically as $g_3\to 0^+$. We study this power-law behavior more carefully near the percolation threshold and we find that the local hydraulic conductance PDF $p(g_3)$ fulfills

$$p(g_3) = Cg_3^{-2/3} \quad \text{for } g_3 \ll 1 \text{ with}$$

$$C(\epsilon,N) = a_\epsilon(N)\epsilon + b_\epsilon(N) \quad \text{or}$$

$$C(A,N) = a_A(N)A + b_A(N) \tag{1}$$

The prefactor C depends on the system size N as well as on the distance to the percolation threshold $\epsilon=p-p_c$. The coefficients a_ϵ, b_ϵ, a_A, and b_A of the linear relations defined in Eq. (1) are given in Table I. This dependence of the bond distribution on the distance to the percolation threshold is a key ingredient which is specific to this problem, and no other studies on similar continuous percolation problems have been found. The following sections show how this dependence significantly affects the behavior of the system.

B. Percolation thresholds

Percolation thresholds p_c and A_c are determined for each of the N_r realizations (see [1] for details). The fraction of percolating realizations $P(X)$ is fitted by the two-parameter error function: $P_{(X_a,\Delta)}(X)=\frac{1}{2}[1+\mathrm{erf}(\frac{X-X_a}{\sqrt{2}\Delta})]$, where variable X is either p or A, and X_a is either p_a or A_a, the averaged percolation thresholds, which tend towards their expected values p_c and A_c for large system sizes (see Table II). As mentioned in [2], behavior of the form $p_a-p_c\sim N^{-1/\nu}$ and $\Delta\sim N^{-1/\nu}$ is expected. Identifications of ν and p_c and A_c can be obtained from these scalings. This yields $\nu\approx 1.57\pm0.02$, $p_c=0.4954$, when p is used to characterize the occupation probability and $\nu\approx 1.48\pm0.02$, $A_c=0.4984$, when A is used. Interpolations from Table IV of [2] yield $\nu\approx 1.40$ and $A_c=0.492$ for $a/l=0.159$ (which is the inverse of the number of points of the surface per correlation length) are indeed consistent with our results. As discussed in detail in [2], the departure from the site percolation standard values ($\nu\approx 1.33$, $A_c=0.40725$) is due to the spatial correlation in the distribution of site—or bond—occupation.

TABLE II. Parameters of percolation probability fits for different system sizes. N_r is the number of realizations.

		$X=A$			$X=p$		
		P_a	Δ	N_r	P_a	Δ	N_r
N	64	46.91	10.32	600	44.87	11.61	600
	128	48.01	6.70	600	46.73	7.87	600
	256	48.94	4.30	600	48.23	5.16	600
	512	49.31	2.63	600	48.90	3.19	600
	1024	49.62	1.59	600	49.54	1.96	600
	2048	49.90	1.03	118	49.88	1.36	57

C. Electrical and hydraulic conductivities

In this section we compute the conductivity exponent with a direct inversion method as described in [1]. For each of the presented results, the computation cost of the transport problem inversion is much smaller than that of calculating the geodesic network. This is why, although other alternatives, such as those proposed in [3,4], could have been used to address the transport problem, it is acceptable to use a standard sparse matrix inversion.

The variation of the electrical conductance associated with the case $n=1$ was computed. A very clear power-law behavior was observed near the percolation threshold, and a power-law fit of the form $G_1=\overline{G_1}\epsilon^t$ led to the values summarized in Table III. The electrical conductivity exponent converges toward the value $t=1.52\pm0.02$ for increasing system size, which is slightly higher than the universal value of 1.3 for 2D systems [see Eq. (2) below]. Very similar estimations of the exponent t were also obtained when considering the electrical conductance variations with A_c-A. The hydraulic conductivity associated with the case $n=3$ is shown in Fig. 2. Here again, the evolution near the percolation threshold is consistent with power-law fits of the form $G_3=\overline{G_3}\epsilon^t$ and $G_3=\overline{G_3}(A_c-A)^t$. The values obtained for the exponent t are presented in Table III for the case where ϵ is the control parameter. As the system size increases, the hydraulic conductance exponent rapidly reaches a constant asymptotic value that was found to be $t=2.8\pm0.05$. The prefactors $\overline{G_1}$ and $\overline{G_3}$ also vary with the system size N and we found $\overline{G_3}\approx 30.1N^{-0.68}$ and $\overline{G_3}\approx 9.8\times10^{-3}N^{-0.65}$ for ϵ and A_c-A as control parameters, respectively. The scale obtained for the conductivity prefactor can be understood if one considers that the red-bond conductivity g^r dominates the conductivity. If N_r is the number of such red bonds, the total conductivity G should scale as $G^{-1}\sim\Sigma_{i=1}^{i=N_r}1/g_i^r$ since red-bond conductivity should be added in series in the nodes-link-blobs picture. Considering that the fractal dimension associated with the red bonds' spatial distribution is $D=3/4$ [5], the red bond number should scale with the system size N as $N_r\sim N^{3/4}$, so that, finally, the conductivity should scale as $G\sim 1/N_r\sim N^{-3/4}$. This prediction is in reasonable agreement with the scaling reported for the conductivity prefactor, which is close to −0.7. The entire PDF of G is also of interest, especially when statistical prescriptions are mandatory. Figure 3 shows the evolution of the PDF of G_3 for several values of ϵ and A. Far

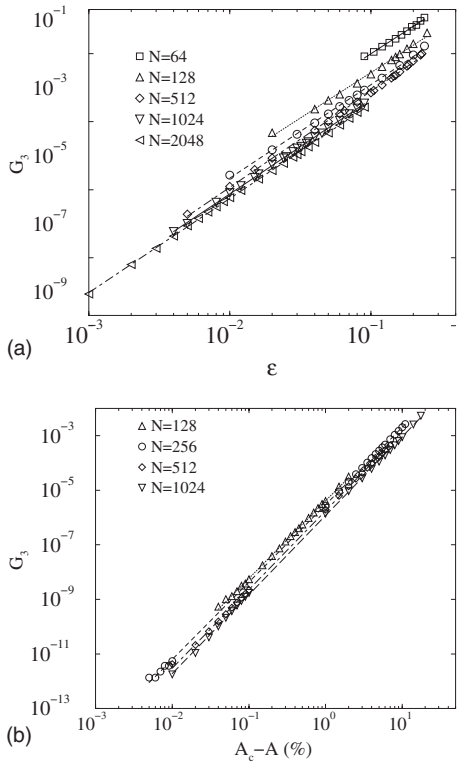

FIG. 2. Evolution of hydraulic conductivity versus ϵ in (a) and $A_c - A$ in (b).

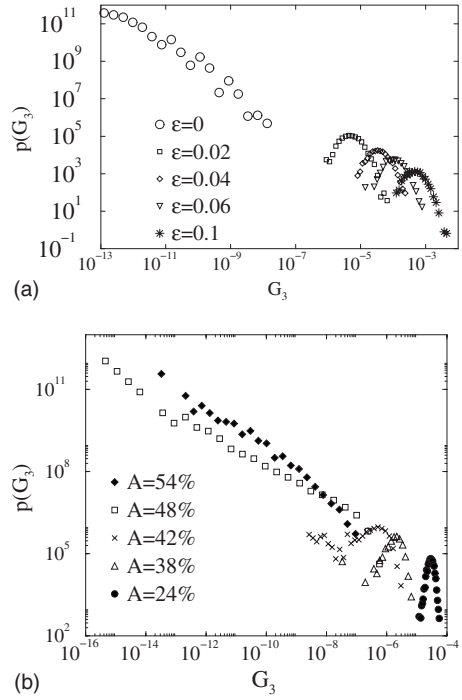

FIG. 3. PDF of G_3 in bilogarithmic coordinates versus ϵ in (a), versus A in (b).

from the percolation threshold it is well represented by a log-normal distribution. In contrast, in the vicinity of the percolation threshold, the PDF of G_3 exhibits a power-law behavior $p(G_3) \sim G_3^{-\beta}$ associated with the lowest values of the conductivity over more than five decades. The estimation of the associated power-law exponent β is between 0.7 and 1 depending on the distance to the percolation threshold.

III. DISCUSSION

This section presents the conductivity exponents obtained in the light of previous studies on continuum percolation [6–10] for which the local conductances g are power-law distributed such that their PDF takes the form $p(g) \sim g^{-\alpha}$, where $0 \leq \alpha \leq 1$. It is now well established [7–10] that the theoretical prediction of the conductivity exponent t of a percolating system is given for a system of infinite size by

$$t = \max[(d-2)\nu + (1-\alpha)^{-1}, t_u], \quad 0 \leq \alpha < 1, \qquad (2)$$

with ν the universal correlation length exponent, d the system dimensionality, and t_u the universal value ($t_u \simeq 1.3$ in 2D [11]). Referring to the conductance distributions of our system, $n=2$ (resp. 3) corresponds to $\alpha = 1/2$ (resp. $2/3$) and Eq. (2) leads to $t = t_u$ (resp. $t=3$), which differs from the values 1.52 ($n=2$) and 2.8 ($n=3$) obtained numerically for our system. As pointed out by Tremblay and Machta (see [6] and references therein) there has been some controversy in the literature about conductance exponents because of their reported finite-size sensitivity. Hence it was interesting to explore the possible influence of finite size effects on the ex-

TABLE III. Exponents of power-law fits of conductivity as a function of system size N for various systems. G_1 and G_3 refer to the electrical and hydraulic conductivities, respectively, of Gaussian fractures. The case G_2 is for a Gaussian fracture with a local conductivity of the form $g_2 \sim h^2(\mathbf{x_s})$. N_r is the number of realizations.

N	G_1		G_2		G_3	
	t	N_r	t	N_r	t	N_r
64	1.3 ± 0.1	400	1.41 ± 0.05	500	2.3 ± 0.1	500
128	1.39 ± 0.05	400	1.61 ± 0.05	300	2.71 ± 0.03	500–1200
256	1.44 ± 0.05	300	1.71 ± 0.02	200	2.74 ± 0.03	1000–2000
512	1.46 ± 0.04	130–180	1.72 ± 0.02	100	2.80 ± 0.01	500–1800
1024	1.49 ± 0.05	119–120	1.75 ± 0.05	50	2.79 ± 0.02	50–250
2048	1.51 ± 0.03	30–52	1.86 ± 0.05	48	2.77 ± 0.01	51–59

TABLE IV. Exponents of power-law fits of conductivity according to system size N for various systems. $\alpha=0,1/2,2/3$ correspond to frozen conductivity distributions $p(g)\sim g^{-\alpha}$.

N	$\alpha=0$		$\alpha=1/2$		$\alpha=2/3$	
	t	N_r	t	N_r	t	N_r
64	0.80 ± 0.05	400	0.94 ± 0.04	500	0.99 ± 0.07	400
128	1.07 ± 0.03	400	1.24 ± 0.04	400	1.26 ± 0.04	400
256	1.20 ± 0.05	300	1.45 ± 0.06	300	1.56 ± 0.1	300
512	1.30 ± 0.02	180–200	1.7 ± 0.1	200–300	2.12 ± 0.05	200
1024	1.34 ± 0.03	119–120	1.8 ± 0.1	50–80	2.29 ± 0.02	100
2048	1.40 ± 0.04	20–40	2.0 ± 0.1	12	2.56 ± 0.02	26

ponents we found for the Gaussian fracture in greater depth. To do so, we also used a frozen power-law distribution of local conductances $p(g_n)\sim g^{-\alpha}$ for specific values of parameter α, i.e., $\alpha=0,1/2,2/3$, which correspond to $n=1,2,3$, respectively. This case is distinct from Eq. (1) where the prefactor of the power law varies with the distance to percolation. The results obtained for the exponent t are summarized in Table IV. It can be observed that, in each case, the measured exponent exhibits a dependence on the finite size which does not saturate even for the largest systems. As previously mentioned, the effective system size is $N/2\pi$, so that $N=2048$ corresponds to a system of approximately 326 correlation lengths. In this case, for $\alpha=0$, the parameter t was found to be equal to 1.40 ± 0.04. Our direct sparse matrix inversion can be compared with the results reported by Tremblay and Machta [6] using a numerical renormalization-group procedure. In two dimensions, they investigated the case $\alpha=0$, for apparent system sizes as large as 10^2 and 10^3, and found apparent exponents of $t=1.42\pm0.02$ and $t=1.49\pm0.02$, respectively, while the theoretical prediction for infinite systems is 1.3 from Eq. (2). Hence our calculation is consistent with their predictions. In the case $\alpha=1/2$, they found $t=2.08\pm0.04$ and $t=1.97\pm0.06$ for apparent system sizes of 10^2 and 10^3, respectively, while we consistently found $t=2.0\pm0.1$ for a system size equal to 326. This validation with previous results confirms that the ideal prediction (2) is rarely relevant for finite size systems. Interestingly, the values reported in Table III reveal that the exponent is much less affected by the finite size effects for the Gaussian fractures than in the case of frozen power-law distributions. This is especially true with $\alpha=2/3$, where the convergence of the asymptotic value $t=2.78\pm0.02$ found for the transport exponent is reached for an effective system size as small as 81. As pointed out, for example, in [12], the conductivity of the system under consideration can be expressed as $G\sim\langle G\rangle\epsilon^{-t_u}$ where $\langle G\rangle$ represents the average value of the link conductance in the system. The nonuniversal contribution to the conductivity exponent $t-t_u$ is determined only by $\langle G\rangle$. Thus the particular behavior of our systems is consistent with the fact that $\langle G\rangle$ behaves differently than with a frozen conductivity distribution because of two distinguishing features. The first one relies on the local conductances variation with the distance to the percolation threshold [cf. Eq. (1)]. The second is the fact that the probability that a bond becomes inactive is not independent of its conductivity in our system.

In addition to the consideration of a new class of continuum percolation, the results presented should be of interest in the context of flows in fractures for which power-law behavior between applied pressure and transport coefficients has been reported experimentally [13].

ACKNOWLEDGMENTS

The research presented in this paper is supported by Grant No. GDR 2345 "Etanchéité statique par joints métalliques en conditions extrêmes" encouraged by CNES, Snecma-Moteur, EDF, and CNRS, and by the "Fondation Charles de Gaulle."

[1] F. Plouraboué, F. Flukiger, M. Prat, and P. Crispel, Phys. Rev. E **73**, 036305 (2006).
[2] V. V. Mourzenko, J. F. Thovert, and P. M. Adler, Phys. Rev. E **53**, 5606 (1996).
[3] Clinton De W. Van Siclen, Phys. Rev. E **59**, 2804 (1999).
[4] Clinton De W. Van Siclen, Phys. Rev. E **65**, 026144 (2002).
[5] A. Bunde and S. Havlin, *Fractals and Disordered Systems* (Springer-Verlag, Berlin, 1991).
[6] A. M. S. Tremblay and J. Machta, Phys. Rev. B **40**, 5131 (1989).
[7] P. N. Sen, J. N. Roberts, and B. I. Halperin, Phys. Rev. B **32**, 3306 (1985).
[8] J. P. Straley, J. Phys. C **15**, 2343 (1982).
[9] B. Berkowitz and G. I. Balberg, Transp. Porous Media **9**, 275 (1992).
[10] P. M. Kogut and J. P. Straley, J. Phys. C **12**, 2151 (1979).
[11] D. Stauffer and A. Aharony, *Introduction to Percolation Theory* (Taylor & Francis, New York, 1992).
[12] C. Grimaldi and I. Balberg, Phys. Rev. Lett. **96**, 066602 (2006).
[13] J. B. Walsh and W. F. Brace, J. Geophys. Res. **89**, 9425 (1984).